A Whole Cell Metal-Organic Framework Encapsulated Vaccine Against Septicemic UPEC Infection.

Michael A. Luzuriaga,[1] Fabian C. Herbert,[1] Olivia R. Brohlin,[1] Arezoo Shahrivarkevishahi,[1] Yalini H. Wijesundara,[1] Kavya Veera,[2] Candace E. Benjamin,[1] Sarah Popal,[1] Michael D. Burton,[3] Molly A. Ingersoll,[5,6] Nicole J. De Nisco,*[,2] and Jeremiah J. Gassensmith*[,1,4]

[1] Department of Chemistry and Biochemistry, [2] Department of Biological Sciences, [3] School of Brain and Behavioral Science, [4] Department of Biomedical Engineering at The University of Texas at Dallas. 800 West Campbel Rd. Richardson, TX 75080 [5] Department of Immunology, Institut Pasteur, Paris, France [6] Inserm U1223, Paris, France

To whom correspondences should be addressed: Nicole.DeNisco@UTDallas.edu and Gassensmith@utdallas.edu

Abstract: Urinary tract infection, most often caused by uropathogenic *Escherichia coli* (UPEC), is the second most common bacterial infection. Rates of antibiotic resistance among UPEC strains is high and front-line antibiotic therapies are losing efficacy. Untreated, UPEC can ascend to the kidneys and into the bloodstream to cause potentially fatal pyelonephritis and bacteremia, respectively. Vaccine development is hampered by the genetic diversity of UPEC strains making selection of antigens capable of inducing broad protection difficult. Whole cell UPEC vaccines offer a solution to the antigen selection problem, however, current inactivation methods are harsh and degrade surface antigens resulting in a weak immune response. Here, we demonstrate a method to gently inactivate whole cell UPEC by encasing them in a crystalline metal-coordination polymeric matrix called a Metal-Organic Framework. This process encapsulates read-to-use composites within 30 minutes in water and at ambient temperatures. We show this new formulation greatly improves survivability in a murine model of UPEC bacteremia compared to standard inactivated formulations. The simplicity of the preparation and use suggests this method could be applied as a point-of-care measure to create therapeutic and prophylactic vaccines against patient derived samples.

Introduction

Development of vaccines against bacterial infection is an ongoing challenge. Globally disseminated antimicrobial resistance (AMR) and the difficulty of developing of antimicrobial agents lacking serious side effects has compelled researchers to look to different strategies to prevent pandemic spread of AMR organisms. AMR is so widespread that treatment of even routine bacterial infections, such as urinary tract infection (UTI), has become problematic.[1] UTIs are the second most common adult bacterial infection worldwide, with ~80% of all community-acquired UTIs caused by uropathogenic *Escherichia coli* (UPEC).[2, 3] Indeed, half of all women will develop a UTI in their lifetime, and more than 40% of these individuals will experience a recurrent infection.[4, 5]

The incidence and recurrent nature of infection take on more urgency given that 10–25% of uncomplicated UTI patient isolates are resistant to trimethoprim/sulfamethoxazole[6, 7] (TMP/SMX), a common antibiotic treatment regimen for UTI. When antibiotic treatment fails, bacteria persist in the bladder, increasing the cost of care and morbidity for the patient.[8] Left untreated, lower UTI can ascend to the kidneys progressing to the more severe diseases of pyelonephritis and urosepsis, which have a global mortality rate of 40%.[9, 10] Given the ubiquity of UTI and the high likelihood of recurrence, the societal cost is estimated to be over $5 billion each year in the US alone.[11] A prophylactic vaccine would be an ideal first line of defense against UTIs but there are no FDA-approved vaccines for this disease.[12] Indeed, no approved vaccine against infection caused by any pathogenic *E. coli* exists.

UPEC presents a unique challenge for the development of vaccines owing to the incredible genetic diversity of UPEC strains, which span the four major phylogenetic groups of *E. coli* (A, B1, B2, D).[13] To create a subunit vaccine, which typically incorporates pathogen surface proteins, the selection of antigens inducing broad protection against all UPECs would be exceedingly difficult. Additionally, subunit vaccines must be conjugated to a carrier to mimic the multivalence found in or on pathogens and require several booster shots to induce a robust immune response.[14, 15] Inactivated, whole cell vaccines

would bypass the need for specific antigen selection required for subunit vaccines. The primary hurdle for the development of inactivated whole cell bacterial vaccines is the weak immune response they elicit because of their short half-life within the body, poor uptake by antigen presenting cells, and surface antigen degradation by harsh fixation methods.[16-18] In the present study, we have developed a method to gently inactivate whole cell bacteria by encasing them in a crystalline metal-coordination polymeric matrix called zeolitic imidazolate framework-8 (ZIF-8). This process occurs within minutes in water, uses inexpensive and biocompatible reagents, occurs at ambient temperatures, and most importantly, greatly improves survivability following systemic bacterial infection compared to standard inactivated formulations.

ZIF encapsulates and inactivates UPEC urosepsis strain CFT073

To develop a whole cell vaccine capable of inducing durable immune responses, we tested whether porous metal-coordination polymers, more commonly known as metal organic frameworks (MOFs), protect surface proteins from denaturation and prolong the release of bacterial antigens. MOFs are low density, crystalline metal-coordination polymers formed from metal nodes that coordinate organic ligands in a highly repeating and ordered matrix (**Figure 1A and B**). These materials are useful in catalysis, separations, sensors, and recently, as non-toxic vehicles for drug delivery.[19-27] We and others have described a specific type of MOF called ZIF-8,[28, 29] composed exclusively of zinc metals interconnected by methylimidazole ligands, that crystallize “biomimetically” on a variety of biomacromolecules including soluble proteins, polysaccharides, viruses, and whole cells. [30-36]

For this study, we used CFT073, a model urosepsis strain of UPEC frequently employed in the development of new vaccines.[37] Gram-negative *E. coli* has an outer membrane containing embedded polysaccharides and proteins,[38-40] which support ZIF-8 growth (**Figure 1C**). We resuspended CFT073 in a saline solution containing 2-methylimidazole (HMIM) and zinc acetate and after washing to remove excess zinc and HMIM, analyzed the resulting encapsulated bacteria, called CFT@ZIF, by scanning electron microscopy (SEM), powder X-ray diffraction (PXRD), and energy dispersive X-ray (EDX)

spectroscopy. ZIF-8 growth occurred exclusively on the surface of the bacteria (**Figure 1D**). The PXRD of CFT@ZIF confirmed the shell was crystalline ZIF-8 (**Figure 1E**) and EDX confirmed the presence of zinc and phosphorus, indicating the presence of both bacteria and ZIF-8 (**Extended Data Fig. 1**).

An initial challenge was the formation of free or empty ZIF-8 crystals. To find conditions that reduced the number of empty ZIF-8 particles (**Figure 1C**, white arrows), we tested a time course of incubation and a range of salinity in the encapsulation solution. We observed that an encapsulation time of 20 minutes and a final concentration of 100 mM NaCl yielded crystal growth primarily on the bacteria (**Extended Data Fig. 2**). Using these parameters to generate CFT@ZIF, we then tested whether we could remove the shells from the encapsulated bacteria, in a process called exfoliation. We observed by transmission electron microscopy (TEM) that the bacteria remained intact after dissolving

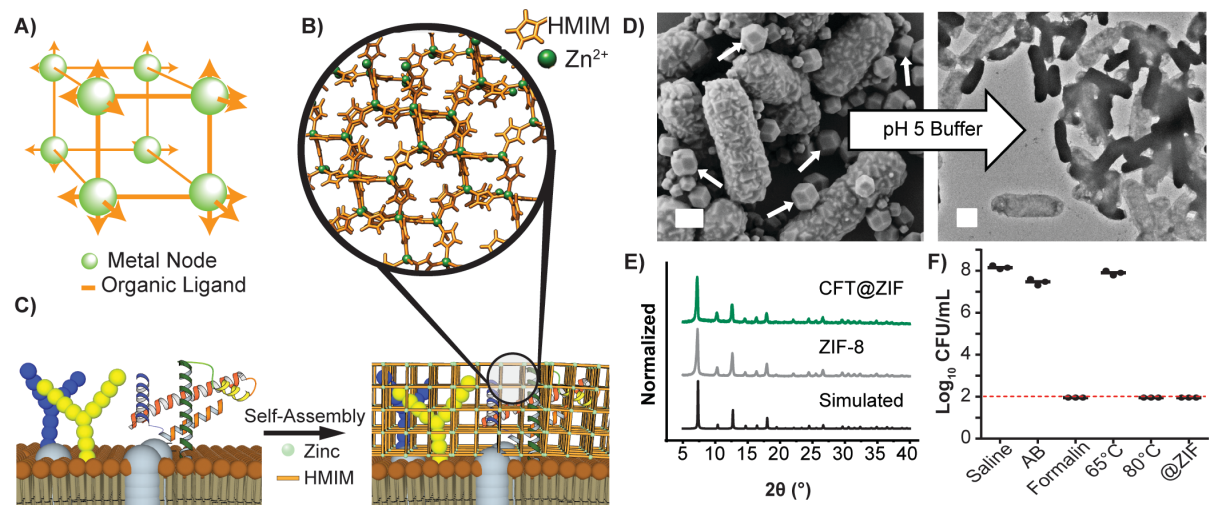

Figure 1: A) Simplified schematic of a metal organic framework composed of metal nodes and organic ligands that can expand infinitely in all directions. B) The crystalline super structure of ZIF-8 is illustrated. C) Conceptualization of the synthetic process shows that the surface of an *E. coli* external membrane can initiate ZIF-8 growth on and around membrane-bound biomacromolecules following incubation with Zn^{2+} and 2-methylimidazole (HMIM). D) Scanning electron micrograph of ZIF-encapsulated UPEC strain CFT073 (CFT@ZIF) (left), which can be removed gently in sodium acetate buffer (AB) at pH 5 to reveal whole bacteria, as seen in the transmission electron micrograph (right). White scale bars are 1 μm and white arrows are free ZIF crystals. E) Powder X-ray diffraction of CFT@ZIF compared to pristine/empty ZIF-8, showing the measured data matches simulated PXRD spectra of pristine ZIF-8. F) Bacteria growth assay shows CFT@ZIF is not viable after exfoliation, similar to formalin fixation or heat treatment, and can be used as a method to inactivate bacteria. The dashed line indicates the detection limit of 100 CFU/mL.

the ZIF-8 shell in mildly acidic (pH 5) sodium acetate buffer and no obvious debris from lysed bacteria were seen (**Figure 1D**).

To assess the stability of the CFT@ZIF, we introduced a plasmid encoding small near-infrared fluorescent protein (smURFP) to CFT073 and monitored smURFP fluorescence of CFT@ZIF and unencapsulated CFT073 during heating (**Extended Data Fig. 3A)**. In addition to finding that thermal stress did not lyse bacteria or induce changes in the CFT@ZIF morphology, we observed that smURFP fluorescence was preserved in CFT@ZIF compared to unencapsulated CFT073 (**Extended Data Fig. 3B)**. We and others reported that ZIF-8 thermally protects proteins immobilized in the ZIF-8 matrix from denaturation,[34, 41-43] likely by limiting conformational mobility within the framework; however, to the best of our knowledge, an example of a protein within a microorganism being protected has not been reported.

A challenge in whole-cell vaccine formulation is that the bacteria must be inactivated with minimal damage to the surface epitopes, including delicate membrane-bound proteins and complex oligosaccharides. We tested whether ZIF encapsulation inactivates CFT073. Following formation of the ZIF shell, immobilized CFT073 was incubated for 30 min at room temperature and exfoliated with 500 mM sodium acetate buffer. Unencapsulated CFT073 was inactivated using formalin or heating as described for other whole-cell bacterial vaccines,[44-46] and bacterial viability was measured for each condition by colony forming unit (CFU) assay, and compared to naked CFT073 incubated in 0.9% saline. Bacterial growth was observed for unencapsulated CFT073 incubated in saline or in the sodium acetate buffer but not for bacteria that were formalin-fixed, heat-inactivated, or, importantly, exfoliated from the ZIF shell (**Figure 1F**). These results support that the ZIF-shell growth process itself inactivates bacteria, which is in line with previous observations that overexposure to zinc causes bacterial cell death.[47-49]

Vaccination with CFT@ZIF induces a robust IgG response

Having established that CFT073 was encapsulated, intact, and inactivated, we turned to immunological studies. A humoral response depends on the activation of antigen-specific

B cells to differentiate into antibody-producing plasma cells.[50] We hypothesized that the ZIF shell would induce higher antibody titers by protecting immunogenic surface antigens. We first compared the time-resolved fluorescence of smURFP-expressing CFT-Fixed, CFT@ZIF, and free ZIF-8 and confirmed that emission was from smURFP within the CFT073 and that formalin fixing did not alter fluorescence *in vivo* (**Extended Data Fig. 3C**). Mice were then injected with saline, formalin-fixed CFT073 (CFT-Fixed), or CFT@ZIF subcutaneously and monitored over a period of 12 days until fluorescence

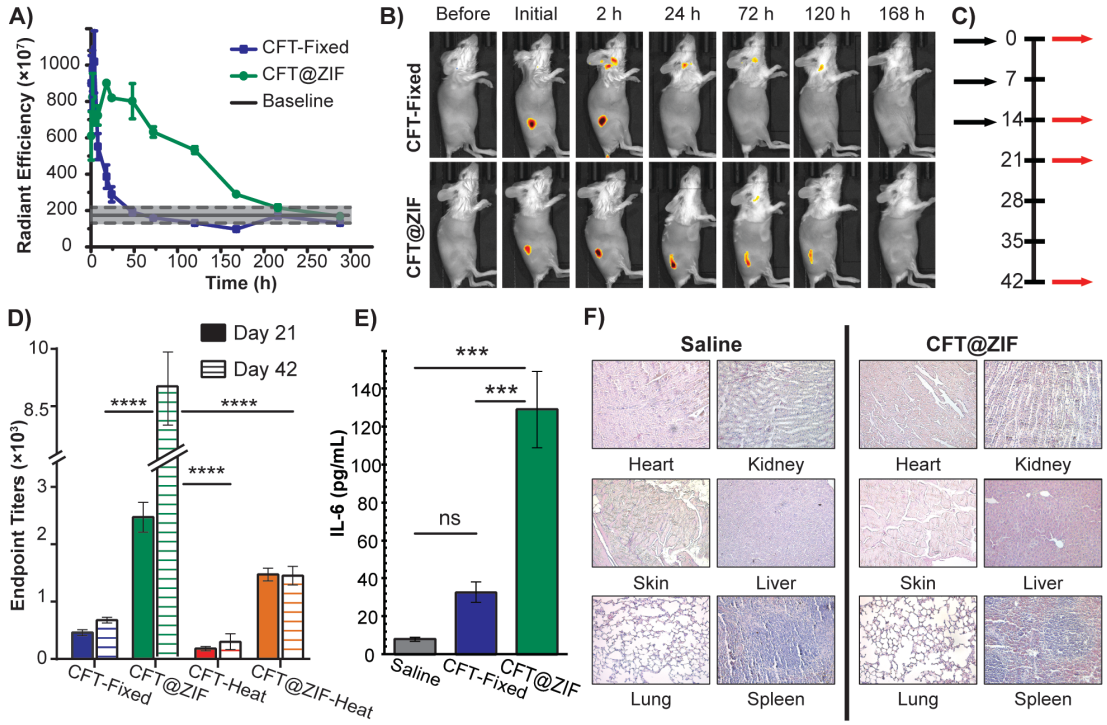

Figure 2: Mice (n=4) were injected with smURFP-expressing CFT073 that was inactivated with formalin (CFT-Fixed) or by encapsulation (CFT@ZIF). A) The graph shows fluorescence change at the site of injection over time. The baseline is the average fluorescence of four mice before and after injecting with saline. The dashed line represents the error of the baseline. B) Representative images of mice prior to injection with CFT-Fixed or CFT@ZIF and after injection were monitored over a course of 12 days. After injection, images were taken at 15, 30, 60, 120, 240, and 480 min, then every 12 h for 12 days. C) Vaccination schedule for mice injected with either saline, CFT-Fixed, CFT@ZIF, CFT-Heat, or CFT@ZIF-Heat. Black arrows are vaccinations and red arrows are blood draws. D) At day 21 and 42, blood was drawn and measured by ELISA to determine the antibody production. E) IL-6 in serum at day 14. F) H&E staining of organs at day 42. Error bars represent the mean±SD. Statistical significance was calculated using an ordinary one-way ANOVA with Tukey's multiple comparison post-test (*$p < 0.05$, **$p < 0.01$, ***$p < 0.0005$, ****$p < 0.0001$).

levels returned to baseline (**Figure 2A**). Images collected during this period show that intact CFT@ZIF remained at the injection site 4 days longer than CFT-Fixed (**Figure 2B**).

We next measured antibody titers in mice injected with saline, CFT-Fixed, thermally inactivated CFT073 (CFT-Heat), CFT@ZIF, or thermally-treated CFT@ZIF (CFT@ZIF-Heat) according to the vaccination and blood sampling schedule in **Figure 2C**. Serum from days 21 and 42 post-injection was serially diluted and the amount of anti-CFT073 IgG produced was determined by ELISA against CFT073. Mice immunized with CFT@ZIF produced the highest levels of anti-CFT073 IgG at day 21 and 42 compared to all other groups (**Figure 2D**). Remarkably, even the thermally stressed CFT@ZIF-Heat induced more anti-CFT073 IgG compared to unstressed CFT-Fixed (**Figure 2D**). As expected, the thermally-inactivated CFT-Heat formulation induced the lowest antibody production, in line with the observation that high temperatures lead to thermal denaturation of proteinaceous and sugar-based epitopes.[51] As IL-6 promotes plasma cell production of immunoglobulins,[52] we diluted serum from day 14 and measured IL-6 production by ELISA. IL-6 levels were highest in CFT@ZIF, which correlated with enhanced production of antibodies in mice injected with this formulation (**Figure 2E**). The increase in CFT073-specific antibodies from mice injected with CFT@ZIF supports the hypothesis that ZIF encapsulation protects immunogenic epitopes. Elevated antibody production may also be a result of the prolonged presence of CFT@ZIF in the tissue compared to unencapsulated bacteria.

Throughout the experiment, mice were monitored daily and showed no signs of pain or changes in behavior, indicating the CFT@ZIF vaccine did not induce acute toxicity. At day 42, the mice were euthanized, and the spleen, liver, kidney, injection site, lung, and heart were collected, fixed in formaldehyde, and stained with H&E for pathological analysis. Organs displayed no signs of toxicity and H&E-stained organ sections showed no abnormal lesions, aggregation, or change in tissue compared to mice injected with saline (**Figure 2F**).

ZIF improves the uptake of CFT073

Antigen persistence via a "depot effect" is correlated with a strong adaptive immune response, as demonstrated above. However, a second mechanistic explanation for the greater antibody response may be increased uptake by professional phagocytes. We hypothesized that coating *E. coli* in a charge-neutral metal-organic framework would promote phagocytosis. ZIF-8 dissolves in the acidic compartments of phagosomes, endosomes, and lysosomes, [53-56] which would free surface epitopes in a manner similar to our exfoliation process in acidic buffer. To test this, we performed ZIF-8 shell growth on smURFP-expressing CFT073 in a solution with GFP to make CFT@ZIF(GFP). The rapid shell formation around the CFT073 serendipitously captured solvated GFP within the crystalline matrix, which created a fluorescent "core-shell" composite that allowed us

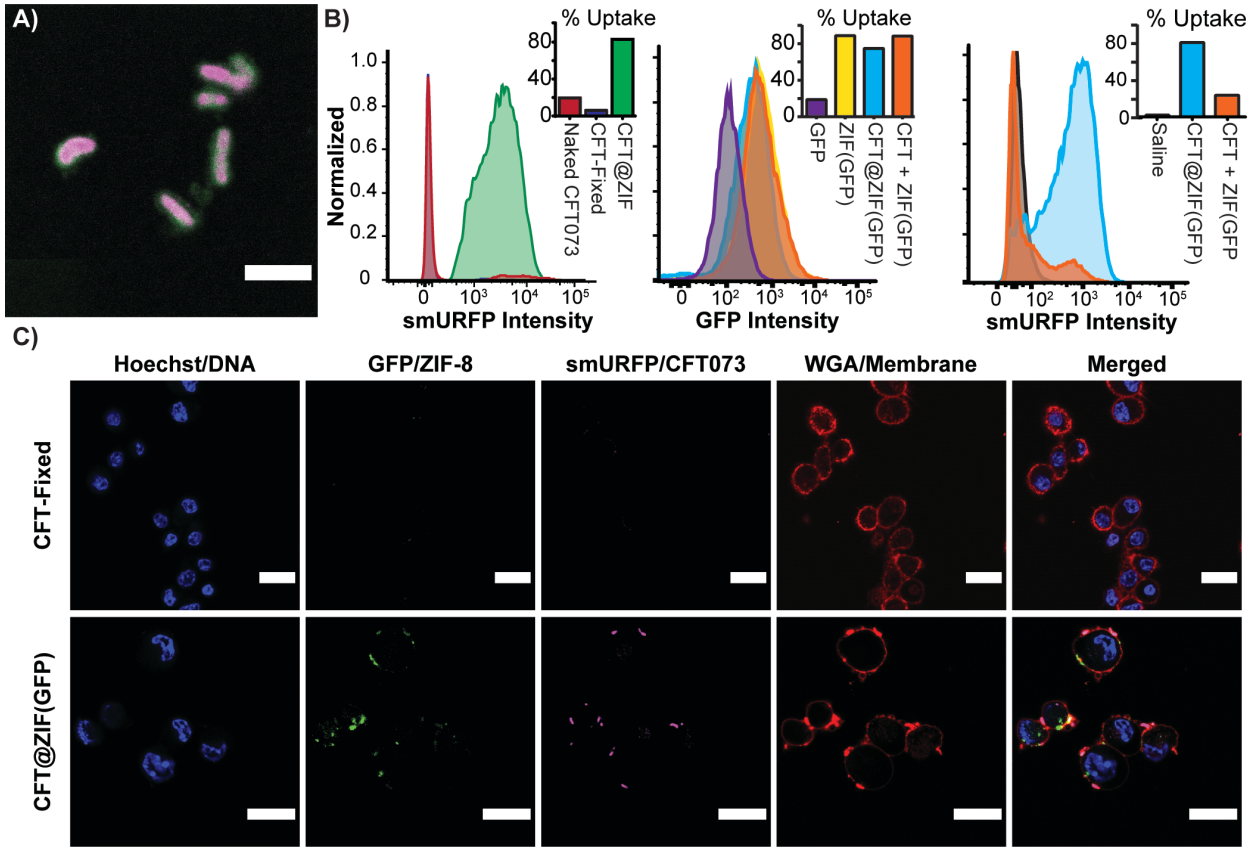

Figure 3: A) Confocal micrograph of CFT@ZIF(GFP). The outer shell fluoresces green from trapped GFP while the encapsulated bacteria fluoresce red. Scale bar = 5 μm. B) Representative histograms show smURFP or GFP fluorescence, for the indicated bacterial preparations and controls. C) Confocal live cell images of smURFP expressing CFT-Fixed and CFT@ZIF(GFP) incubated with RAW 264.7 macrophages after 4 h. Scale bar = 20 μm.

to monitor the bacteria separately from the ZIF shell (**Figure 3A**). CFT073, CFT-Fixed, and CFT@ZIF(GFP) were incubated for four hours with RAW 264.7 macrophages. Flow cytometry analyses showed a four-fold increase in uptake of ZIF formulations of CFT073 over naked CFT073 and more than an order of magnitude increase over formalin-fixed CFT (**Figure 3B**). Confocal microscopy images revealed that GFP was taken up by the cells, which strongly indicates that the ZIF-shell was intact during bacterial uptake (**Figure 3C**). To rule out that the presence of ZIF-8 in the media promoted macrophage phagocytosis, a mixture of CFT073 and ZIF-8 crystals (CFT+ZIF(GFP)) was incubated together with the macrophages, which did not result in greater CFT073 uptake compared to naked CFT073. Taken together, these data demonstrate that the ZIF encapsulation is correlated with increased uptake of CFT073. This, in addition to the depot effect, likely accounts for the strong antibody response observed in **Figure 2D**.

Vaccination with CFT@ZIF enhances a cell-mediated response and protects mice from lethal sepsis challenge

Activation of a cell-mediated immune response is a vital aspect of vaccine development to promote long-term memory.[57, 58] To determine whether CFT@ZIF promotes a cell-mediated immune response, we measured TNF-α, an immunostimulatory cytokine mainly produced by macrophages and T_h1 (Type 1 T helper) $CD4^+$ T cells, and IFN-γ, a cytokine produced mainly by T_h1 T cells and dendritic cells promoting a cell-mediated response by stimulating cytotoxic T lymphocytes.[59, 60] We employed the vaccination schedule depicted in **Figure 2C**, and on day 21, re-stimulated splenocytes collected from each group with CFT073. We measured TNF-α (**Figure 4A**) and IFN-γ expression (**Figure 4B**) levels by ELISA, observing that mice immunized with CFT@ZIF had higher levels of both cytokines compared to CFT-Fixed treated mice following re-stimulation. Taken together, our data indicate a more robust cell mediated response in mice treated with CFT@ZIF compared to CFT-Fixed-vaccinated mice.

Mice vaccinated with CFT@ZIF had increased antibody production and increased expression of multiple key cytokines at day 21 compared to other CFT formulations. To

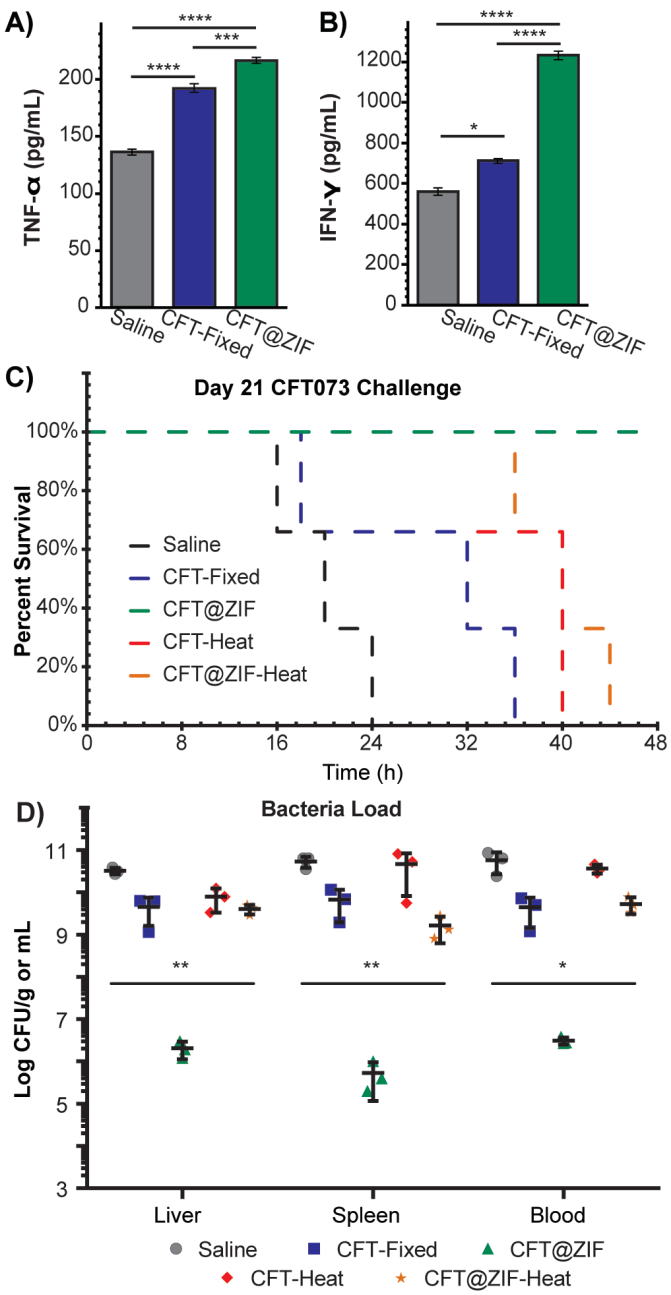

Figure 4: Mice (n=4) were injected with CFT073 that was inactivated with formalin (CFT-Fixed) or by encapsulation (CFT@ZIF). At Day 21, splenocytes were collected from immunized mice and incubated with 10 µg/mL of naked CFT073 for 48 h. After 48 h, the supernatant was tested for A) TNF-α and B) IFN-γ. A second cohort of mice following the vaccination schedule in **Figure 2C** were injected interperitoneally with a lethal dose of CFT073 at day 21 and monitored for 48 h. C) Survival for each group over the course of 48 h. D) When the mice became moribund or by the end of 48 h were assessed for the bacteria loads in the liver, spleen, and blood. Error bars represent the mean±SD. Statistical significance was calculated using an ordinary one-way ANOVA with Tukey's multiple comparison post-test (*$p < 0.05$, **$p < 0.01$, ***$p < 0.0005$, ****$p < 0.0001$).

determine whether these responses would be protective, we used a uro-sepsis model.

We vaccinated as above with either saline, CFT-Fixed, CFT-Heat, CFT@ZIF, or thermally stressed CFT@ZIF. On day 21, we administered a lethal dose[15] of CFT073 and mice were monitored over the course of 48 hours and euthanized when they became moribund, defined by lack of movement for over 15 minutes, shaking in place, and a decrease of body temperature. All CFT@ZIF-vaccinated mice survived after 48 hours compared to the other treated groups, which all succumbed to challenge (**Figure 4C**). After euthanasia, blood, spleens, and livers were collected, homogenized, and CFUs were enumerated (**Figure 4D**). Bacterial load in the blood, spleens, and livers of CFT@ZIF-vaccinated mice were four orders of magnitude lower than all the other groups. This lower bacterial load may be attributed to the 5-fold higher anti-CFT073 IgG that CFT@ZIF promotes over CFT-Fixed. Notably, the thermally stressed CFT@ZIF formulation promoted longer survival, which hints at a possible thermally protective effect of the ZIF-8 shell, an observation that is with considerable precedence.[61-63]

Conclusion

In this work, we demonstrated that ZIF-8 effectively inactivated a urosepsis strain of UPEC, creating a persistent vaccine formulation that considerably outperformed current whole cell inactivation methods in nearly every regard. This method of inactivation avoids the use of toxic formaldehyde, and is faster, more convenient, and yields superior results. Only CFT@ZIF-vaccinated mice survived a lethal dose of CFT073, which we attribute to the five-fold increase in IgG and superior uptake by phagocytes as compared to CFT-Fixed-vaccinated mice. Furthermore, this reduction in bacterial load and survival exceeds the efficacy of published subunit vaccine strategies for CFT073.[8, 64, 65] The results showing improved survival even after thermally stressing the vaccine formulation are in line with published data showing that ZIF protects surface epitope structure. Finally, the biomimetic growth strategy that we employed here is likely generalizable across a number of different organisms, presenting an enormous opportunity for a generalizable approach toward whole-cell vaccine formulation. Formulation of the inactivated bacteria does not use dangerous or toxic compounds, involves the mixture of only three components, and the total reaction time is under 30 minutes. Our ecologically friendly and low-cost approach makes it an ideal platform for rapid vaccine production from patient isolate UTIs.

This creates an opportunity to produce rapidly patient-specific prophylactic and therapeutic vaccine formulations for those suffering from recurrent UTI in a truly personalized medicine approach.

References

1. Sugianli, A.K. et al. Antimicrobial resistance in uropathogens and appropriateness of empirical treatment: a population-based surveillance study in Indonesia. *J. Antimicrob. Chemother.* **72**, 1469-1477 (2017).
2. Kabbani, M. & Kramer, M. in Urology at a Glance. (eds. A.S. Merseburger, M.A. Kuczyk & J.W. Moul) 157-160 (Springer Berlin Heidelberg, Berlin, Heidelberg; 2014).
3. Terlizzi, M.E., Gribaudo, G. & Maffei, M.E. UroPathogenic Escherichia coli (UPEC) infections: Virulence factors, bladder responses, antibiotic, and non-antibiotic antimicrobial strategies. *Front. Microbiol.* **8**, 1566-1566 (2017).
4. Foxman, B. Epidemiology of urinary tract infections: Incidence, morbidity, and economic costs. *DM, Dis.-Mon.* **49**, 53-70 (2003).
5. Neugent, M.L., Hulyalkar, N.V., Nguyen, V.H., Zimmern, P.E. & De Nisco, N.J. Advances in understanding the human urinary microbiome and its potential role in urinary tract infection. *mBio* **11**, e00218-00220 (2020).
6. Majeed, A., Alarfaj, S., Darouiche, R. & Mohajer, M. An update on emerging therapies for urinary tract infections. *Expert Opin. Emerging Drugs* **22**, 53-62 (2017).
7. Hooton, T.M. Recurrent urinary tract infection in women. *Int. J. Antimicrob. Agents* **17**, 259-268 (2001).
8. Mellata, M., Mitchell, N.M., Schödel, F., Curtiss, R. & Pier, G.B. Novel vaccine antigen combinations elicit protective immune responses against Escherichia coli sepsis. *Vaccine* **34**, 656-662 (2016).
9. Artero, A. et al. Prognostic factors of mortality in patients with community-acquired bloodstream infection with severe sepsis and septic shock. *J. Crit. Care* **25**, 276-281 (2010).
10. Labelle, A. et al. The determinants of hospital mortality among patients with septic shock receiving appropriate initial antibiotic treatment*. *Crit. Care Med.* **40**, 2016-2021 (2012).
11. Foxman, B. Urinary tract infection syndromes: occurrence, recurrence, bacteriology, risk factors, and disease burden. *Infect. Dis. Clin. N. Am.* **28**, 1-13 (2014).
12. Asadi Karam, M.R., Oloomi, M., Mahdavi, M., Habibi, M. & Bouzari, S. Vaccination with recombinant FimH fused with flagellin enhances cellular and humoral immunity against urinary tract infection in mice. *Vaccine* **31**, 1210-1216 (2013).
13. Farajzadah Sheikh, A. et al. Virulence-associated genes and drug susceptibility patterns of uropathogenic Escherichia coli isolated from patients with urinary tract infection. *Infect. Drug Resist.* **12**, 2039-2047 (2019).
14. Bachmann, M.F. et al. The influence of antigen organization on B cell responsiveness. *Science* **262**, 1448-1451 (1993).
15. Vartak, A. & Sucheck, S.J. Recent advances in subunit vaccine carriers. *Vaccines* **4**, 12 (2016).
16. Blackburn, N.K. & Besselaar, T.G. A study of the effect of chemical inactivants on the epitopes of Rift Valley fever virus glycoproteins using monoclonal antibodies. *J. Virol. Methods* **33**, 367-374 (1991).

17. Shaw-Wei, D.T. et al. Chemical-free inactivated whole influenza virus vaccine prepared by ultrashort pulsed laser treatment. *J. Biomed. Opt.* **20**, 1-8 (2014).
18. Frey, J. Biological safety concepts of genetically modified live bacterial vaccines. *Vaccine* **25**, 5598-5605 (2007).
19. Huxley, M.T. et al. Protecting-group-free site-selective reactions in a metal–organic framework reaction vessel. *J. Am. Chem. Soc.* **140**, 6416-6425 (2018).
20. Otake, K.-I. et al. Single-atom-based vanadium oxide catalysts supported on metal–organic frameworks: Selective alcohol oxidation and structure–activity relationship. *J. Am. Chem. Soc.* **140**, 8652-8656 (2018).
21. Hayashi, H., Côté, A.P., Furukawa, H., O'Keeffe, M. & Yaghi, O.M. Zeolite A imidazolate frameworks. *Nat. Mater.* **6**, 501-506 (2007).
22. Li, L. et al. Highly efficient separation of methane from nitrogen on a squarate ‐ based metal ‐ organic framework. *AIChE Journal* **64**, 3681-3689 (2018).
23. Fan, C. et al. Silver nanoclusters encapsulated into metal–organic frameworks with enhanced fluorescence and specific ion accumulation toward the microdot array-based fluorimetric analysis of copper in blood. *ACS Sens.* **3**, 441-450 (2018).
24. Zhuang, J. et al. Optimized metal–organic-framework nanospheres for drug delivery: evaluation of small-molecule encapsulation. *ACS Nano* **8**, 2812-2819 (2014).
25. Adhikari, C., Das, A. & Chakraborty, A. Zeolitic imidazole framework (ZIF) nanospheres for easy encapsulation and controlled release of an anticancer drug doxorubicin under different external stimuli: a way toward smart drug delivery system. *Mol. Pharmaceutics* **12**, 3158-3166 (2015).
26. Zheng, H. et al. One-pot synthesis of metal–organic frameworks with encapsulated target molecules and their applications for controlled drug delivery. *J. Am. Chem. Soc.* **138**, 962-968 (2016).
27. Abánades Lázaro, I. et al. Selective surface PEGylation of UiO-66 nanoparticles for enhanced stability, cell uptake, and pH-responsive drug delivery. *Chem* **2**, 561-578 (2017).
28. Li, S. et al. Investigation of controlled growth of metal–organic frameworks on anisotropic virus particles. *ACS Appl. Mater. Interfaces* **10**, 18161-18169 (2018).
29. Riccò, R. et al. Metal–organic frameworks for cell and virus biology: A perspective. *ACS Nano* **12**, 13-23 (2018).
30. Hoop, M. et al. Biocompatibility characteristics of the metal organic framework ZIF-8 for therapeutical applications. *Appl. Mater. Today* **11**, 13-21 (2018).
31. Wang, C. et al. Metal–organic framework encapsulation for biospecimen preservation. *Chem. Mater.* **30**, 1291-1300 (2018).
32. Zhang, Y. et al. Metal ‐ Organic ‐ Framework ‐ Based Vaccine Platforms for Enhanced Systemic Immune and Memory Response. *Adv. Funct. Mater.* **26**, 6454-6461 (2016).
33. Astria, E. et al. Carbohydrates@MOFs. *Mater. Horiz.* **6**, 969-977 (2019).
34. Li, S. et al. Template ‐ directed synthesis of porous and protective core ‐ shell bionanoparticles. *Angew. Chem., Int. Ed.* **55**, 10691-10696 (2016).
35. Liang, K. et al. Metal–organic framework coatings as cytoprotective exoskeletons for living cells. *Adv. Mater.* **28**, 7910-7914 (2016).
36. Li, S. et al. Hierarchical porous carbon arising from metal–organic framework-encapsulated bacteria and its energy storage potential. *ACS Appl. Mater. Interfaces* **12**, 11884-11889 (2020).
37. Kaper, J.B., Nataro, J.P. & Mobley, H.L.T. Pathogenic Escherichia coli. *Nat. Rev. Microbiol.* **2**, 123-140 (2004).
38. Spurbeck, R.R. et al. Fimbrial profiles predict virulence of uropathogenic Escherichia coli strains: contribution of ygi and yad fimbriae. *Infect. Immun.* **79**, 4753-4763 (2011).

39. Alteri, C.J., Hagan, E.C., Sivick, K.E., Smith, S.N. & Mobley, H.L.T. Mucosal immunization with iron receptor antigens protects against urinary tract infection. *PLoS Pathog.* **5**, e1000586 (2009).
40. Moriel, D.G. et al. Identification of protective and broadly conserved vaccine antigens from the genome of extraintestinal pathogenic Escherichia coli. *Proc. Natl. Acad. Sci. U. S. A.* **107**, 9072-9077 (2010).
41. Zhang, H., Chen, W., Gong, K. & Chen, J. Nanoscale Zeolitic Imidazolate Framework-8 as Efficient Vehicles for Enhanced Delivery of CpG Oligodeoxynucleotides. *ACS Appl. Mater. Interfaces* **9**, 31519-31525 (2017).
42. Alsaiari, S.K. et al. Endosomal Escape and Delivery of CRISPR/Cas9 Genome Editing Machinery Enabled by Nanoscale Zeolitic Imidazolate Framework. *J. Am. Chem. Soc.* **140**, 143-146 (2018).
43. Liang, K. et al. Biomimetic mineralization of metal-organic frameworks as protective coatings for biomacromolecules. *Nat. Commun.* **6**, 7240 (2015).
44. Jalava, K., Hensel, A., Szostak, M., Resch, S. & Lubitz, W. Bacterial ghosts as vaccine candidates for veterinary applications. *J. Controlled Release* **85**, 17-25 (2002).
45. Torres, J.F., Lyerly, D.M., Hill, J.E. & Monath, T.P. Evaluation of formalin-inactivated Clostridium difficile vaccines administered by parenteral and mucosal routes of immunization in hamsters. *Infect. Immun.* **63**, 4619-4627 (1995).
46. Sunwoo, H.H., Lee, E.N., Menninen, K., Suresh, M.R. & Sim, J.S. Growth inhibitory effect of chicken egg yolk antibody (IgY) on escherichia coli O157:H7. *J. Food Sci.* **67**, 1486-1494 (2002).
47. Couñago, R.M. et al. Imperfect coordination chemistry facilitates metal ion release in the Psa permease. *Nat. Chem. Biol.* **10**, 35-41 (2014).
48. Velasco, E. et al. A new role for zinc limitation in bacterial pathogenicity: modulation of α-hemolysin from uropathogenic Escherichia coli. *Sci. Rep.* **8**, 6535 (2018).
49. McDevitt, C.A. et al. A molecular mechanism for bacterial susceptibility to zinc. *PLoS Pathog.* **7**, e1002357 (2011).
50. Pape, K.A., Catron, D.M., Itano, A.A. & Jenkins, M.K. The humoral immune response is initiated in lymph nodes by B cells that acquire soluble antigen directly in the follicles. *Immunity* **26**, 491-502 (2007).
51. Welch, R.P., Lee, H., Luzuriaga, M.A., Brohlin, O.R. & Gassensmith, J.J. Protein–polymer delivery: Chemistry from the cold chain to the clinic. *Bioconjugate Chem.* **29**, 2867-2883 (2018).
52. Tanaka, T., Narazaki, M. & Kishimoto, T. IL-6 in inflammation, immunity, and disease. *Cold Spring Harbor Perspect. Biol.* **6**, a016295 (2014).
53. Chen, T.-T., Yi, J.-T., Zhao, Y.-Y. & Chu, X. Biomineralized metal-organic framework nanoparticles enable intracellular delivery and endo-lysosomal release of native active proteins. *J. Am. Chem. Soc.* **140**, 9912–9920 (2018).
54. Sun, C.-Y. et al. Zeolitic imidazolate framework-8 as efficient pH-sensitive drug delivery vehicle. *Dalton Trans.* **41**, 6906-6909 (2012).
55. Durymanov, M. et al. Cellular uptake, intracellular trafficking, and stability of biocompatible metal-organic framework (MOF) particles in kupffer cells. *Mol. Pharmaceutics* **16**, 2315-2325 (2019).
56. Zhong, X. et al. An aluminum adjuvant-integrated nano-MOF as antigen delivery system to induce strong humoral and cellular immune responses. *J. Controlled Release* **300**, 81-92 (2019).
57. Obst, R. et al. Sustained antigen presentation can promote an immunogenic T cell response, like dendritic cell activation. *Proc. Natl. Acad. Sci. U. S. A.* **104**, 15460-15465 (2007).
58. Demento, S.L. et al. Role of sustained antigen release from nanoparticle vaccines in shaping the T cell memory phenotype. *Biomaterials* **33**, 4957-4964 (2012).
59. Spellberg, B. & Edwards, J.E., Jr. Type 1/Type 2 immunity in infectious diseases. *Clin. Infect. Dis.* **32**, 76-102 (2001).

60. Natarajan, K. et al. The role of molecular flexibility in antigen presentation and T cell receptor-mediated signaling. *Front. Immunol.* **9**, 1657 (2018).
61. Wang, C. et al. Metal-organic framework encapsulation preserves the bioactivity of protein therapeutics. *Adv. Healthcare Mater.* **7**, 1800950 (2018).
62. Luzuriaga, M.A. et al. Enhanced stability and controlled delivery of MOF-encapsulated vaccines and their immunogenic response in vivo. *ACS Appl. Mater. Interfaces* **11**, 9740-9746 (2019).
63. Liang, W. et al. Control of structure topology and spatial distribution of biomacromolecules in protein@ZIF-8 biocomposites. *Chem. Mater.* **30**, 1069-1077 (2018).
64. Durant, L. et al. Identification of candidates for a subunit vaccine against extraintestinal pathogenic Escherichia coli. *Infect. Immun.* **75**, 1916-1925 (2007).
65. Sidjabat, H.E. et al. Colonisation dynamics and virulence of two clonal groups of multidrug-resistant Escherichia coli isolated from dogs. *Microbes and Infection* **11**, 100-107 (2009).

Acknowledgements

This project was partially funded by The University of Texas at Dallas Office of Research through the SPIRe grant program. J.J.G. thanks the National Science Foundation [CAREER DMR-1654405] and the Welch Foundation [AT-1989- 20190330]. The Gassensmith Lab would like to thank the University of Texas at Dallas lab animal resource center (LARC) for mouse maintenance. We especially like to thank Tyler Tornblom and Bradly Woody from LARC for the mice training they provided. C.E.B. thanks the National Science Foundation Graduate Research Fellows Program (1746053).

Author Contribution

Primary manuscript writing and editing was done by M.A.L., M.A.I. N.J.D. and J.J.G. Cytokine ELISA, body clearance, SEM, EDX, flow cytometry, and survival challenge were done by M.A.L. Mouse injections and blood draws were done by M.A.L. and F.C.H. TEM imaging was done by O.R.B. Confocal images were taken by O.R.B. and C.E.B. PXRD was done by Y.W. smURFP induction was done by K.V. Histological analysis was done by A.S. Antibody ELISA was done by S.P. Flow prep was done by M.A.L., A.S., and O.R.B. ZIF optimization was done by M.A.L. and F.C.H. Bacteria growth and killing assay was done by F.C.H. Immunological studies were aided by M.D.B. Funding was raised by N.J.D. and J.J.G.

Competing Interest

The authors declare no competing interest